ISTITUTO NAZIONALE DI FISICA NUCLEARE

Sezione di Milano

INFN/TC-90/11
9 Maggio 1990

L. Serafini, M. Ferrario, C. Pagani, A. Peretti:

SHOK: SUB-HARMONIC HIGH-GAIN OPTICAL KLYSTRON

Servizio Documentazione
dei Laboratori Nazionali di Frascati

INFN - Istituto Nazionale di Fisica Nucleare
Sezione di Milano

INFN/TC-90/11
9 Maggio 1990

SHOK: SUB-HARMONIC HIGH-GAIN OPTICAL KLYSTRON

L. Serafini, M. Ferrario, C. Pagani, A. Peretti
INFN and Università di Milano - Via Celoria 16 - 20133 Milano

ABSTRACT

A new method for pumping a single passage high gain FEL is presented, based on the exploitation of a sub-harmonic input signal which drives the start up of the exponential gain on the fundamental harmonic of the wiggler. Significant gain enhancements can be obtained: furthemore, the advantage of the SHOK scheme is very pronounced in the VUV soft X-ray domain, where no coherent input signal is available at such short radiation wavelengths, since it allows to employ the comon available UV laser beams as input signal for a XUV FEL.

1 - INTRODUCTION

One of the main open problem in the operation of FEL-s and Optical Klystrons within the short wavelength domain is the difficulty to find a suitable coherent signal (i.e. a laser beam) to be used as the input radiation field for the FEL amplifier[1]. Being straightforward that a VUV X-ray FEL must be a single passage amplifier[2] (due to the lacking of efficient mirrors in this frequency range), an input signal is needed to be injected into the wiggler and amplified via the high gain FEL mechanism, based on a strong coupling between the wiggle electron beam motion and the radiation field. The best results, in term of coherence and output power of the radiation field, are obtained with a coherent input signal with same radiation wavelength as the fundamental resonating wavelength of the selected wiggler-beam system [3].

In the SASE (Self Amplified Spontaneous Emission) mode of operation the input signal is directly the incoherent spontaneous emission produced by the beam because of its transverse motion in the wiggler. The field power of the spontaneous emission radiation scales with the beam current I and with the square of the beam energy γ^2: it can easily reach some tens of kW per meter of wiggler[7], for wiggler-beam systems tuned to radiate in the X-VUV range. Whenever the high gain conditions are satisfied by the beam-wiggler system, the exponential growth of the self-amplified radiation sets up and the field power (at saturation) comes out to scale[4] like $I^{4/3}$ (whenever the superradian effects[5] are negligible). The advantage of the SASE mode is that no input signal is required: however the coherence of the output signal is lower. The coherence length of the output signal produced in the SASE regime is indeed given roughly by the slippage length: since the electrons interact with one another via the common radiation field, the interaction length is equal to the slippage length, hence the photons separated by more than the slippage length are of course decoupled. Therefore, the start up of the field amplification process from photon and electron populations which are both randomly distributed in phase cannot assure a narrow bandwidth and a coherent output signal.

Some frequency multiplication scheme have been recently proposed to avoid this difficulty [6,7]: they essentially consist of a double (planar) wiggler cascade in which the fundamental harmonic of the second wiggler is tuned at the same frequency as one of the higher (odd) harmonics of the first wiggler. At the passage between the two wigglers a jump in frequency is obtained by a factor 3 or 5: the advantage is clearly that the coherent input signal injected at the entrance of the first wiggler is lower in frequency than the radiated field at the output of the whole system. Hence, laser beams available in the UV range can be converted in the X-VUV range and amplified up to high peak powers level[7] (some hundrets of MW). However, such schemes have the disadvantage to require two different (and in some cases separate) wigglers, fact that strongly increases the un-reliability of the whole system and all the problems related to beam-radiation phase mis-matching, beam transport, wiggler tolerances, etc. Moreover, high frequency multiplication factors cause a relevant gain decrease in the second wiggler because of the induced energy spread by the first wiggler on its fundamental harmonic, which is seen as an incoherent energy spread by the fundamental harmonic of the second wiggler[8]: theefore the frequency multiplication cannot be higher than a factor 3 or 5 if the FEL performances need to be saved.

In this paper we present a scheme of frequency multiplication operating with only one wiggler, requiring no input signal nor on the fundamental neither on higher hamonics and an unbunched beam at the wiggler entrance, i.e. a device capable to start up the exponential gain process on the fundamental harmonic just from the equilibrium condition of zero field and zero bunching. This device is based simply on a sub-harmonic signal injection: under proper conditions, the subharmonic coherent input signal is capable to induce a modulation in the beam energy (i.e. a coherent energy spread) which is converted into a bunching by the wiggler dispersive action.

The first section is devoted to illustrate the extension of the FEL Compton equations to the presence of a sub-harmonic field wave and to present some general results obtained by the numerical integration.

The second section presents a first possible application of the SHOK scheme to drive a FEL in the VUV range, to obtain coherent radiation at a wavelength of 40 nm with a peak power of some hundrets of MW.

The last section presents the possibility to reach the so-called "water window" at 5 nm of radiation wavelength via the exploitation of an extended SHOK scheme.

Both the experiments should be feasible within the context of the ARES[17] project - as presented in the "ARES Design Study" -, which anticipates the design and construction of a SC LINAC able to produce high brightness electron beams in the 400-800 MeV range.

2 - The SHOK scheme

The break up of the equilibrium condition of zero field and unbunched beam, which is a stable fixed point for the FEL equations, is achieved via the injection of a sub-harmonic input signal, matched to the electron beam, into the wiggler. This signal can be a laser beam at a suitable frequency being a sub-multiple of the fundamental resonant wavelength of the wiggler-beam system. We called such a device, which is simply a sub-harmonic assisted wiggler, Sub-Harmonic Optical Klystron, because, as in the standard optical klystron configuration[9], an input laser beam is employed to stimulate a bunching of the injected beam on the scale of the resonant radiation wavelength. Once a small but finite bunching is achieved, if the proper conditions are met to operate the FEL in the high gain regime, the exponential growth of the radiated field naturally sets up according to the standard steady state behaviour of the FEL amplification process.

The driving effect of the sub-harmonic input signal, which has a wavelength $\lambda_s = s \cdot \lambda_r$ (s is the sub-harmonic index and λ_r is the fundamental resonant wavelength of the wiggler), consists essentially in inducing a coherent energy modulation onto the electron beam: such an energy spread is transformed by the wiggler, which can be viewed as a dispersive medium, into a phase modulation, i.e. a density modulation. Therefore the beam comes out to be bunched on the scale of the sub-harmonic wavelength λ_s and on all the higher harmonics: in particular the harmonic of wavelength λ_r is just the bunching component of interest to start up the FEL amplification process on the resonant wavelength λ_r.

Let us examine now how a sub-harmonic signal of wavelength λ_s, injected into a wiggler of period λ_w at the same time of an electron beam of energy γ, can induce a modulation in energy of the beam on the scale of its wavelength λ_s. The resonant wavelength λ_r is given by the usual FEL resonance relationship:

$$\lambda_r = \frac{\lambda_w (1 + a_w^2)}{2 \gamma^2 n}$$

where n is an odd integer number (n=1 gives the fundamental first harmonic radiated by the beam while n>1 gives the higher resonating harmonics) and a_w is the dimensionless vector potential of the wiggler. In a planar wiggler a_w is related to the peak magnetic field, B_w, by the formula: $a_w \approx .66\,\lambda_w$ [cm] B_w [T].

We define an electromagnetic field for the sub-harmonic laser beam in a similar way as for the higher harmonics:

$$\vec{E_s}(z,t) = \frac{mc^2}{e}\frac{\hat{x}}{\sqrt{2}}\,(\tilde{e}_s(z,t)\,e^{i(kz-\omega t)/s} + c.c.) \qquad 1)$$

where $\tilde{e}_s$ is a slowly varying complex amplitude that, using the SVEA approximation, can be derived from a vector potential $\tilde{a}_s = a_s\,e^{i\phi s}$, such that $|\tilde{e}_s| = k\cdot a_s$, using $E=-(1/c)\partial/\partial t(mc^2\tilde{a}_s/e)$.

The normalized transverse velocity of an electron injected in a planar wiggler is given, neglecting the effects due to the electromagnetic wave and to the betatron motion, by[10]:

$$\vec{\beta_\perp} = \sqrt{2}\,\frac{a_w}{\gamma}\cos(k_w z)\,\hat{x} \qquad 2)$$

where $k_w = 2\pi/\lambda_w$ and $\hat{x}$ gives the transverse horizontal direction of a planar wiggler extending longitudinally along z.

The work done by the sub-harmonic field on the wiggling electron, on the basis of the Lorentz energy equation, comes out to be[*]:

$$\left(\frac{d\gamma}{dz}\right)_s = -\,2\,\frac{ka_wa_s}{\gamma}\cos\left(\frac{kz-\omega t}{s}+\phi_s\right)\cos(k_w z) \qquad 3)$$

The complete energy equation, including the radiative harmonics contribution, becomes:

$$\frac{d\gamma}{dz} = -\,2\sum_{h}^{h\,odd}\frac{ka_wa_h}{\gamma}\cos[h(kz-\omega t)+\phi_h]\cos(k_w z) + \left(\frac{d\gamma}{dz}\right)_s \qquad 3\text{-b})$$

where a_h is the vector potential amplitude of the h-th harmonic.

In order to satisfy the SVEA approximation[11] it is usual to average over a wiggler period the fast oscillations induced in the energy equation by the planar magnetostatic field structure. In presence of a sub-harmonic field the averaging must be performed over $s\cdot\lambda_w$, i.e. over a number of wiggler periods equal to the sub-harmonic order s. Defining $\theta = (k_w+k)z - \omega\bar{t}$ as the average electron phase over a wiggler period (or, equivalently, over s wiggler periods), where $\bar{t} = (z/c)\cdot(1+(1+ a_w^2/2\gamma^2))$ is the averaged arrival time, the actual electron phase, which takes into account the fast oscillations, comes out to be given by $\theta_f = \theta - \xi\sin(2k_w z)$, where the parameter ξ

---

[*] The contribution due to the betatron motion can be neglected whenever the betatron wavelength λ_b is much larger than the wiggler period λ_w. Since $\lambda_b/\lambda_w = \sqrt{2}\cdot\gamma\cdot H/a_w$, for the case of X-VUV FEL's this ratio is >>1.

is defined as $\xi = ka_w^2/(4k_w\gamma^2)$ and, if the electron γ is close to the resonant γ_r, it depends only on the wiggler potential a_w, i.e. $\xi = a_w^2/2(1+a_w^2)$.

The averaged energy equation can then be written as

$$\overline{\left(\frac{d\gamma}{dz}\right)}_s = -2\frac{ka_w}{\gamma s\lambda_w}\int_{z-s\lambda_w}^{z} a_s \cos\left[\frac{\theta}{s} - \frac{k_w z'}{s} - \frac{\xi}{s}\sin(2k_w z') + \phi_s\right]\cos(k_w z')\,dz' \qquad 4)$$

Assuming that the electron phase θ remains constant over the averaging period $s\cdot\lambda_w$, it is easy to see that the integral in 4) is vanishing whenever the amplitude a_s of the sub-harmonic field is constant over $s\cdot\lambda_w$: no energy spread can be induced with a sub-harmonic field whose intensity stays constant along the wiggler. In fact, the energy spread contributions produced at each half of a wiggler period are summed along s wiggler periods to give exactly zero. Taking as an example the sub-harmonic of order two (s=2), it is easy to figure out that the electron beam sweeps away one sub-harmonic wavelength, with respect to the sub-harmonic optical field wave, every two wiggler periods: therefore, each electron of the beam, independently of its phase, experiences, at each wiggler period, two opposite, but equal in amplitude, momentum transfers (corresponding to the two halves wiggler period). The total momentum transfer on the electron will be therefore exactly zero.

There is, however, a possibility to avoid such an exact compensation and get a not-vanishing total momentum transfer, as sketched in Fig.1: if the sub-harmonic field is given by a single mode laser beam of wavelength λ_s injected into the wiggler from an external source, the optical field amplitude on axis will be given by

$$\left|\vec{E}\right| = \frac{\left|\vec{E_0}\right|}{\sqrt{1+\frac{z^2}{Z_0^2}}} \qquad 5)$$

where w_0 is the spot at the beam waist and Z_0 is the Rayleigh range $Z_0 = \pi w_0^2/\lambda_s$. Since the transverse distribution of the optical field amplitude is gaussian ($|E(r)| = |E(r=0)|\cdot e^{-(r/w)^2}$), the overlap between the electron beam (with transverse gaussian distribution of width σ) and the laser beam requires $w_0 = \sqrt{2}\sigma$ (**), fixing the Rayleigh range at $Z_0 = 2\pi\sigma^2/\lambda_s$. The integral on the r.h.s. in 4) is not vanishing if the variation of the sub-harmonic field is significant over one wiggler period λ_w: the Rayleigh range Z_0 must be therefore not too large with respect to λ_w.

(**) The wiggle motion of the electron beam can perturb the overlap with the sub-harmonic laser beam: the ratio between the amplitude of the wiggle motion and the rms beam radius can be extimated to be given by $(x_{max}/\sigma) = .01.B_w^{3/2}[T]/(\sqrt{\varepsilon_n H}.\gamma)$. In our case this ratio is always « 1, indicating that the overlap can be considered complete.

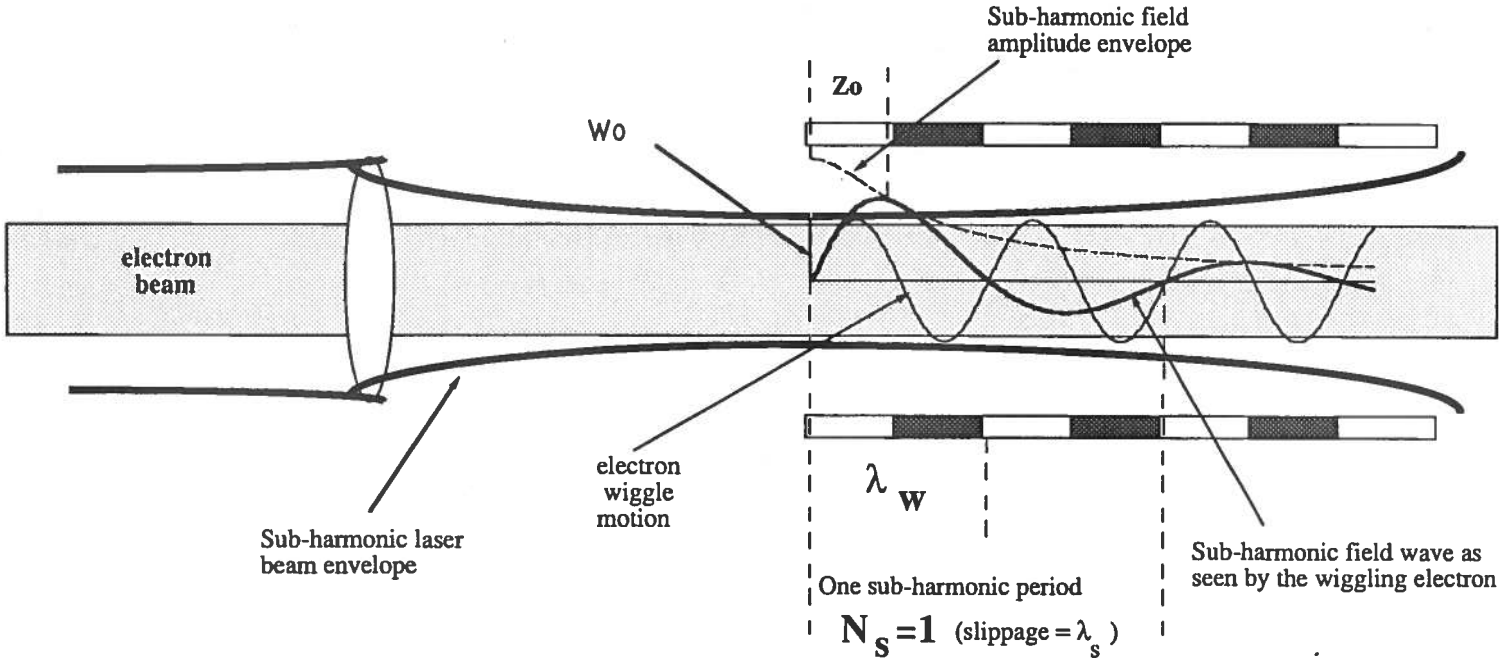

Fig.1 - Schematics of a second order s=2 sub-harmonic beam-field coupling

Taking the usual scaling low for the beam radius in a wiggler with appropriate shaping of the pole face[12] one can compute that the ratio Z_0/λ_w is given by:

$$\frac{Z_0}{\lambda_w} = \frac{\gamma}{\sqrt{2}\,\pi\, s}\,\frac{H}{a_w} \qquad 6)$$

where H is the fractional reduction of the betatron wavelength due to the amount of ion focussing applied[13] (H=1 no ion focussing). For electron beams of some hundrets of MeV and a sub-harmonic index s in the range 3-5 a ratio Z_0/λ_w in the order of some tens can be achieved: that implies a not-vanishing integral on the r.h.s. of eq. 4), i.e. the possibility to induce an energy spread in the electron beam using a sub-harmonic input signal.

We will examine later on the efficiency of such a process, after the insertion of the sub-harmonic field action in the FEL Compton equations[14], as described in the following.

The complex vector potential $\tilde{a}_s$ of the sub-harmonic field can be redefined and set in a dimensionless form introducing the new variables[11,15]:

$$A_s = \frac{\omega}{\omega_p\sqrt{\rho\gamma_r}}\,\tilde{a}_s$$

$$p_j = \frac{\gamma_j - \gamma_r}{\rho\gamma_r} \qquad 7)$$

$$\bar{z} = 2\,k_w \rho\, z$$

where ρ is the Pierce parameter $\rho=(1/\gamma)(a_w\omega_p/4ck_w)^{2/3}$, ω_p is the beam plasma frequency $\omega_p = \sqrt{4\pi e^2 n/m_o}$ (n is the electron beam density), γ_j is the gamma of the j-th electron and γ_r the resonant gamma. We recall that the complex dimensionless field amplitude A_s is expressed as $A_s = |A_s|e^{i\phi_s}$, where $\rho|A_s|^2$ gives the ratio between the energy density of the sub-harmonic laser beam and the electron beam energy density. Assuming, at the wiggler entrance, a perfect overlap between the electron beam and the sub-harmonic laser beam, the initial value of $|A_s|^2$ at z=0 will be given by $|A_s^0|^2 = P_s/(\rho P_b)$, where P_s is the sub-harmonic laser beam power and P_b the electron beam power.

Expressed in the dimensionless units the momentum equation 3), which accounts for the energy spread induced by the sub-harmonic field, becomes:

$$\left(\frac{dp_j}{d\bar{z}}\right)_s = \dot{p}_j^s \equiv -\chi(\bar{z})\frac{|A_s^0|}{\sqrt{1+\frac{\bar{z}^2}{\bar{Z}_0^2}}}\cos\left[\frac{\theta_j}{s}-\frac{\bar{z}}{2\rho s}-\frac{\xi}{s}\sin\left(\frac{\bar{z}}{\rho}\right)+\phi_s\right]\cos\left(\frac{\bar{z}}{2\rho}\right) \qquad 8)$$

$$\text{with} \quad \chi(\bar{z}) = \begin{cases} 0 & \bar{z}<0 \\ 1 & \bar{z}\geq 0 \end{cases}$$

where we recall that θ_j is the electron phase averaged over a wiggler period. The function $\chi(\bar{z})$ is needed to take into account a semi-infinite wiggler starting from $\bar{z}=0$: the sub-harmonic field action given in eq.3) starts indeed at the wiggler entrance, $\bar{z}=0$.

Since the coupling between the electron beam and the sub-harmonic field is very low, as will be shown later on, we will assume the sub-harmonic field as an external driving force whose variation in time and space is specified by the optical behaviour of the sub-harmonic laser beam, as given in eq.1), with an optical field amplitude as specified in eq.5).

Inserting the contribution to the energy spread coming from the sub-harmonic field into the FEL Compton equations we get:

$$\begin{aligned} \frac{dp_j}{d\bar{z}} &= -\sum_{h\ odd} F_h(\xi)(A_h e^{ih\theta_j} + c.c.) + \dot{p}_j^s \\ \frac{d\theta_j}{d\bar{z}} &= p_j \qquad\qquad j = 1,N \qquad\qquad 9) \\ \frac{dA_h}{d\bar{z}} &= F_h(\xi)\langle e^{-ih\theta_j}\rangle \qquad \text{where} \quad \langle\ \rangle \equiv \frac{1}{N}\sum_{j=1}^{N} \end{aligned}$$

where the term $b_h = \langle e^{-ih\theta_j}\rangle$ is usually called the bunching parameter on the h-th harmonic. The coupling coefficients $F_h(\xi)$ are given by[14] $F_h(\xi) = J_{(h-1)/2}(h\xi) - J_{(h+1)/2}(h\xi)$.

Averaging the first of the eqs. 9) over the N electrons, using also the third one, we get:

$$\frac{d}{d\bar{z}}\left(\langle p\rangle + \sum_{h}^{h\ odd}|A_h|^2\right) = \langle \dot{p}^s\rangle \qquad 10)$$

which states that the total momentum associated to the electron beam and to the odd radiative harmonics (on the r.h.s. of eq.10), which, in absence of the sub-harmonic field, is a well known constant of the motion, varies along the wiggler until the sub-harmonic field is able to exchange momentum to the electron beam, i.e. until $\langle \dot{p}^s\rangle \neq 0$.

Looking at eq.8), it comes out that the work done by the sub-armonic field onto the beam electrons becomes vanishing for $\bar{z} \gg \bar{Z}_0$, implying that the momentum exchange $\langle p^s \rangle$ from the sub-armonic field to the electron beam reaches, after an initial transient regime, a constant value, given by

$$\langle p \rangle + \sum_{h}^{h\ odd} |A_h|^2 = \langle p^s \rangle \equiv \int_0^{\bar{z}} \langle \dot{p}^s \rangle d\bar{z}' \qquad 11)$$

The new constant of the motion becomes $\langle p \rangle + \Sigma_h |A_h|^2 - \langle p^s \rangle = 0$, in the case of zero detuning and zero field amplitude at the wiggler entrance. It will be shown later that the final momentum exchange between the electron beam and the sub-harmonic field, i.e. the quantity $\langle p^s \rangle$ evaluated at $\bar{z} \gg \bar{Z}_0$, is negligible with respect to the final value of $\langle p \rangle$ at saturation, which is of the order of 1.

Therefore, we can explain the effect of the sub-harmonic field on the system formed by the beam and the radiative harmonics in terms of a driven shift of the system away from the equilibrium condition $b_h=0$ and $A_h=0$, applied during a transient regime which lasts a few units of $\bar{Z}_0$. It can be seen at a glance that the codition $b_h=0$ and $A_h=0$ is no more a fixed stable point for the system of eq. 9): if the term p_j is modulated over the phase space with a non-zero first harmonic component, i.e. if $\langle p_j \cdot e^{i\theta j} \rangle \neq 0$, a uniform beam ($b_h=0$) in absence of any starting signal ($A_h=0$) will get a phase modulation, i.e. a bunching, as given by: $\dot{b} = i \langle p_j \cdot e^{i\theta j} \rangle$, which can be deduced by the 2nd of eq. 9). It comes out that the action of the sub-harmonic field is the breaking of the stable equilibrium condition of zero field and zero bunching. The new stable equilibrium condition becomes, for the eq. 9), $b_h=0$, $A_h=0$ and $A_s^0=0$ (or $Z_0 \dashrightarrow \infty$, i.e. a parallel laser beam).

In order to study the excitation of the exponential regime on the first and the higher harmonics of the wiggler, starting with a uniform beam and zero first harmonic signal ($A_1 = 0$), we integrated numerically the system of equations 9) using some hundrets (tipically 720) of macroparticles to simulate the electron beam. The macroparticles are initially distributed with $p_j=0$ and with phases θ_j uniformly distributed over $2\pi s$ radians in the phase space: the bucket of the sub-harmonic field is indeed extending over s buckets of the first harmonic, hence the phase space will have a periodicity of order $2\pi s$.

As a first test we pointed out our attention to the lowest sub-harmonic index, s=2, the second order sub-harmonic. The free parameters are in our case the amplitude of the sub-harmonic field at the wiggler entrance, $|A_s^0|$, the Rayleigh range of the sub-harmonic laser beam Z_0 and the wiggler potential a_w. We chose a typical value for $a_w = 1.5$, corresponding to a wiggler period $\lambda_w = 2$ cm and B = 1.1 T, a ratio $Z_0/\lambda_w = 10$ and an initial sub-harmonic field amplitude $|A_s^0| = 0.15$. The quantity $\bar{Z}_0$ is defined as $\bar{Z}_0 = 4\pi\rho \cdot (Z_0/\lambda_w)$. Taking for ρ a typical value $\rho=.002$, we have $\bar{Z}_0 = .25$.

The phase variation for a particle started at (θ=.035 rad, p=0) is plotted in Fig.2 versus $\bar{z}$ from $\bar{z}$=0. to $\bar{z}$=1., which corresponds to 40 wiggler periods. The small oscillations (of the order of $1 \cdot 10^{-5}$ rad) of the electron phase θ confirm that this is slowly varying along the wiggler and represents just the average electron phase over one wiggler period. Note that the fast electron phase θ_f exhibits fast oscillations over one wiggler period with amplitude ξ (which is of the order of 1). The phase space trajectory is shown, for the same particle, by the solid line plotted in Fig.3: the scalloped shape of the trajectory clearly shows that the electron undergoes relevant oscillations in momentum accompanied by small oscillations in phase (note the enlarged scale in abscissa). The dashed line in the same figure connects the points of the trajectory corresponding to the end of each wiggler period: the fast oscillations induced by the sub-harmonic field are washed out and only a slowly varying phase shift is left. It must be noted that in the numerical integration the step has been taken small with respect to the wiggler period (i.e. $\delta\bar{z} \ll 4\pi\rho$) in order to take into account the fast oscillations in p.

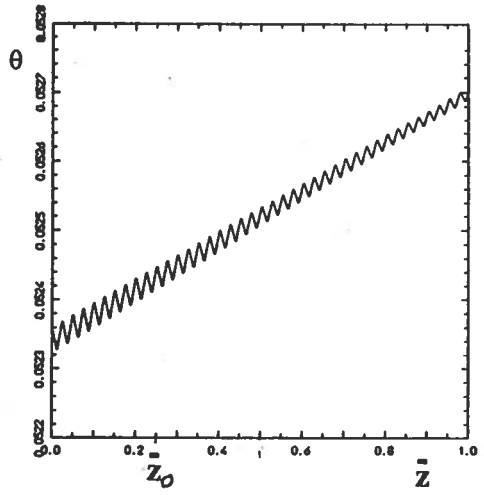

Fig.2 - Behaviour of the average electron phase θ plotted as a function of $\bar{z}$, for a test particle.

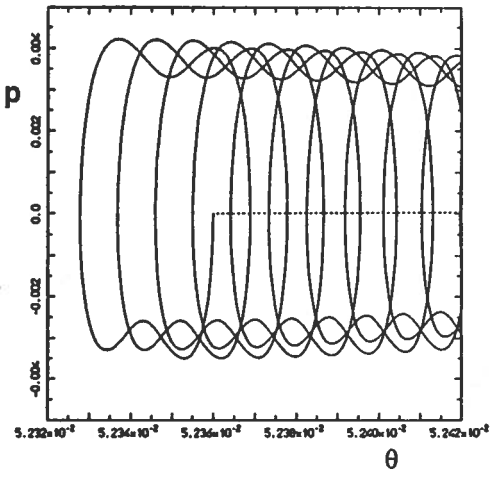

Fig.3 - Phase space trajectory of the same particle of Fig.2, starting at $\bar{z}$=0 from θ=.05236 rad, p=0.

The maximum value of p over the phase space p_{max} (i.e. the amplitude of the beam energy modulation over a sub-harmonic wavelength, recalling that p is the normalized energy spread) is plotted in Fig.4 (solid line) as a function of $N_s = \bar{z}/(4\pi\rho s)$. Since at each wiggler period λ_w the electrons shift by one first harmonic wavelength λ_r with respect to the first harmonic field wave, a number s of wiggler periods are needed to produce a slippage of one sub-harmonic wavelength $\lambda_s = s\lambda_r$ with respect to the sub-harmonic field wave. Then, the quantity N_s gives the number of sub-harmonic wavelengths seen by the beam, or, equivalently, the slippage in units of λ_s. The position of Z_0 on this scale is also shown in abscissa at $N_s(Z_0) = Z_0/s\lambda_w = 5$. The phase space is shown in Fig.5 after one half of the first wiggler period (dotted line) and after two wiggler periods (bolded line), i.e. at N_s=1. The phase space range is $2s\pi$ = 12.57 rad.

In Fig.4 the action of the sub-harmonic field is clearly visible: recalling that the number of wiggler periods are, for this case of s=2, just doubled with respect to N_s, it can be seen that the maxima in the energy modulation amplitude are reached at half of each wiggler period, with an

envelope following just the laser beam intensity behaviour. The minima are initially positioned at the end of each wiggler period: for a constant average electron phase θ the integral in 4) gives always a minimum at $z=n\lambda_w$, and the minimum value is exactly zero if the sub-harmonic laser beam envelope is parallel, i.e. the optical field on axis is constant. The value of the minima is instead growing along the wiggler and their position shifts slowly just after the end of each wiggler period, due to the slow variation of the average electron phase θ, as shown by the dashed line plotted in Fig.4, which connects the values of the energy modulation amplitude at the end of each wiggler period: the asympthotic value of this curve, which is quickly reached at some Z_0 units, gives just the final amplitude of the energy modulation induced by the sub-harmonic laser beam. At that point the sub-harmonic intensity can be considered really negligible and no more active on the electron beam.

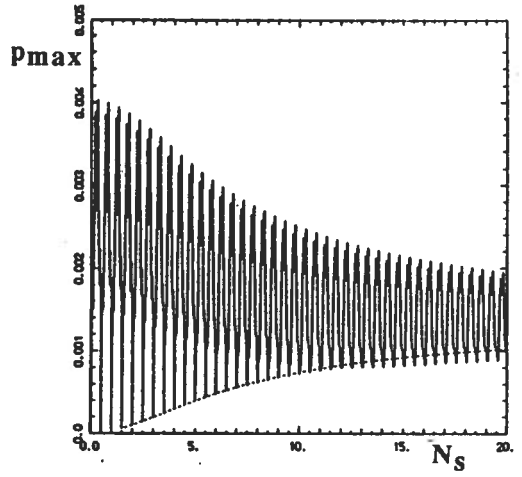

Fig.4 - Maximum p over the phase space (i.e. amplitude of the energy modulation) plotted (solid line) along 40 wiggler periods, i.e. N_S=20. The dashed line connects the values assumed at the end of each wiggler period. See text for details.

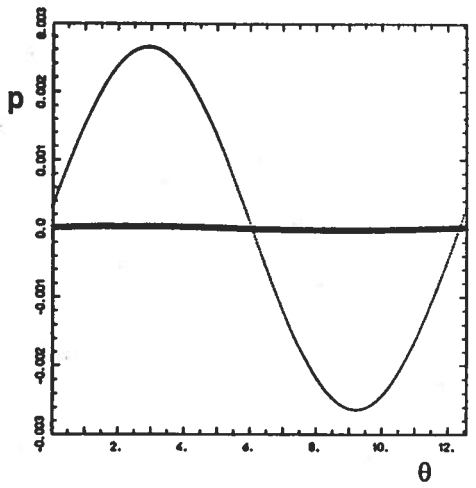

Fig.5 - Phase spaces of the 720 simulating particles traced at the end of the first wiggler period (dotted line) and at the end of the second wiggler period (bolded line), where N_S=1. See text for details.

It is not so surprising that the asymptotic value of the final amplitude of the energy modulation does not depend (to the first order) on the value of Z_0/λ_w. Indeed, neglecting the slow variation of θ over a few units of Z_0, the total momentum transfer can be derived by an integral similar to that in eq.4) extended from z=0 up to $z=nZ_0$ (n small): the maximum over the phase space (θ=0-2π) scales linearly with $|A_S^0|$ (i.e. with the initial amplitude of the sub-harmonic optical field) and scales invariant with Z_0. That is confirmed by the curves plotted in Fig.6: the solid line shows the maximum value of p over the phase space at the end of each wiggler period, from N_S=0 up to N_S=160 (i.e. along 320 wiggler periods), obtained with a value of Z_0/λ_w = 10, while the dashed line is given by a value of Z_0/λ_w = 20 and the dotted line by Z_0/λ_w = 80. The asympthotic value reached by the two curves is substantially the same.

The total momentum transfer $\langle p_S \rangle$ between the sub-harmonic field and the electron beam is plotted (for the case Z_0/λ_w=20) in Fig.7 as a function of $\bar{z}$ from the wiggler entrance up to $\bar{z}$=6., which corresponds to 240 wiggler periods. The momentum transfer is negative, implying that the

electron beam looses energy, but its value is very small ($\approx -2 \cdot 10^{-9}$), hence the coupling between the sub-harmonic field and the electron beam is very weak. The momentum transfer from the electron beam to the sub-harmonic field (which should gain energy) is therefore negligible when compared to the sub-harmonic field intensity variation caused by the optical laser beam behaviour.

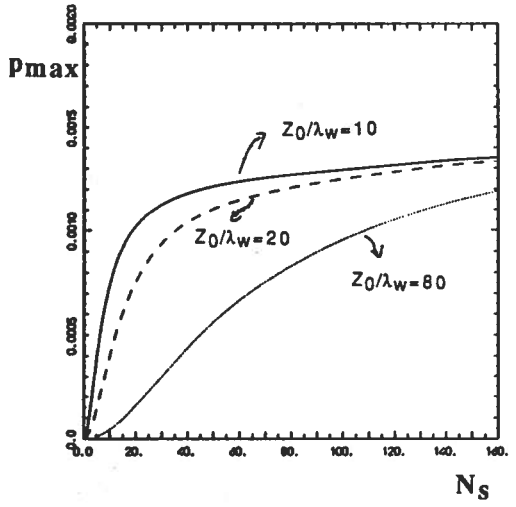

Fig.6 - Maximum p over the phase space plotted at the end of each wiggler period, over 320 wiggler periods (i.e. N_S=160), for three different values of Z_0/λ_w, as indicated. See text for details.

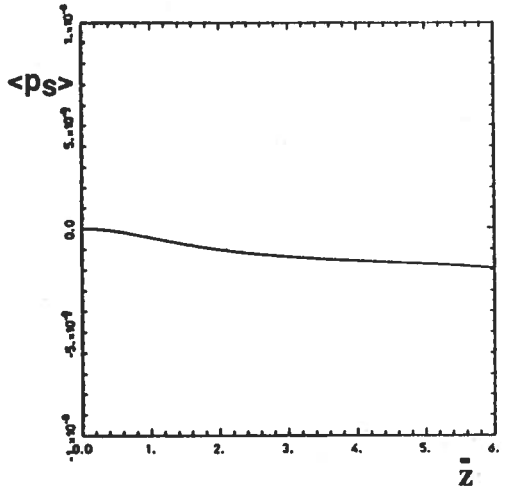

Fig.7 - Momentum transfer $\langle p_S \rangle$ between the sub-harmonic field wave and the electron beam, plotted as a function of $\bar{z}$. See text for details.

To summarize, we list the following main results:

- the sub-harmonic field can induce a coherent energy spread whenever the intensity of the sub-harmonic signal is varying monotonically along the wiggler: the final energy spread scales linearly with the difference between the initial amplitude of the sub-harmonic signal (at the wiggler entrance) and its final amplitude (which is nearly zero for a defocussing optical laser beam matched with the electron beam at the wiggler entrance). Other type of sub-harmonic signals can be considered, within different spectral region: for instance, guided microwave pulses within linearly tapered wave-guides could be used as sub-harmonic signals for FEL's in the microwave region.

- the evolution of the sub-harmonic field along the wiggler is mainly determined by the optical properties of the laser beam, since the coupling with the electron beam is very weak: the sub-harmonic field produces essentially an energy modulation with a very low energy absorption from the electron beam ($\langle p_S \rangle$ negative and very small, like in a very low gain regime).

- the quantity $\langle p \rangle + \Sigma_h |A_h|^2$, which is the usual constant of the motion in absence of the external driving force due the sub-harmonic field, is still constant just after an initial transient regime: the energy exchange between the electron beam and the radiative harmonics is not perturbed by the presence of the sub-harmonic field inducing the energy modulation since the total momentum

transfer between the electron beam and the sub-harmonic field is negligible with respect to the coupling between the electron beam and the radiative harmonics.

- the average electron phase θ is still a slowly varying quantity, with very low residual oscillations over a wiggler period

- the final amplitude of the coherent energy spread induced by the sub-harmonic field does not depend (to a good approximation) from the Rayleigh range Z_0, i.e. from the actual shape of the laser beam envelope (this seems to be valid for Z_0 not so much high with respect to the wiggler period).

The perfomances of the SHOK scheme can be deduced from the evolution of the first harmonic field intensity along the wiggler starting from a condition of zero field ($|A_1|^2=0$). Fixing the input parameters at the values indicated above we continued the integration of eq. 9) versus $\bar{z}$ varying the initial amplitude of the sub-harmonic field, namely with the three different values $|A_s^0|^2$ = .2, .02, .002.

We used an integration step equal to one hundreth of a wiggler period, i.e. $\delta\bar{z} = 4\pi\rho/100$, and a double precision calculation, i.e. a machine epsilon ε_m around $1\cdot10^{-15}$: that implies a noise level on the initial bunching of the same order, since the "uniform" distribution of the particles in the initial phase space (at $\bar{z} = 0$) suffers for a straggling in the θ position of each particle which is equal to the machine epsilon. Therefore, the start up of the exponential regime in the first harmonic is unavoidable, as can be seen in Fig.8, where the bolded line mark the growth of the first harmonic normalized field intensity (the logarithm $\log|A_1|^2$ is plotted) versus $\bar{z}$.

The numerical noise in the phase space drives initially the field intensity which grows very fast, until the bunching, caused by the noise, reaches an equilibrium regime with the radiated field intensity (at $\bar{z}\approx2$): at that point the standard exponential behaviour sets in and the field continues to grow exponentially till the saturation is reached at $\bar{z}\approx50$, with a field intensity $|A_1|^2 \approx 1$. The behaviour of the bunching amplitude $|b_1|$ is plotted in Fig.9, where the dashed line marks the quantity $\log|b_1|$ as a function of $\bar{z}$. The bunching stays fairly constant at the initial value up to the point where the radiated field has grown enough to create a potential well in which the particles are trapped in: at that point also the bunching starts to grow exponentially (its log increases linearly).

The evolution of the logarithm of the field intensity $\log|A_1|^2$ in presence of an injected sub-harmonic signal is plotted in Fig.8: the dotted line is given by an initial $|A_s^0|^2 = 0.002$, the dashed line corresponds to $|A_s^0|^2 = 0.02$ and the solid line to $|A_s^0|^2 = 0.2$, while the behavior of the quantity $\log|b_1|$ is plotted in Fig.9 (solid line) just for the case $|A_s^0|^2 = 0.2$.The strong driving effect applied to the bunching by the sub-harmonic field is clearly evident: the energy spread induced by the sub-harmonic field is converted by the wiggler into a phase modulation, hence in a bunching, as specified by the phase equation for θ_i in the system 9). The first harmonic field reaches the saturation after $\bar{z}\approx20$ starting from a zero initial amplitude. The first plotted value, which specifies

the lowest level of the scale at -38, is just the value of $\log|A_1|^2$ after the first integration step: this value $|A_1|^2 \approx 3.10^{-38}$ is given just by the numerical noise in the phase space, i.e. by the initial bunching, and is indeed the same for all the lines plotted in Fig.8.

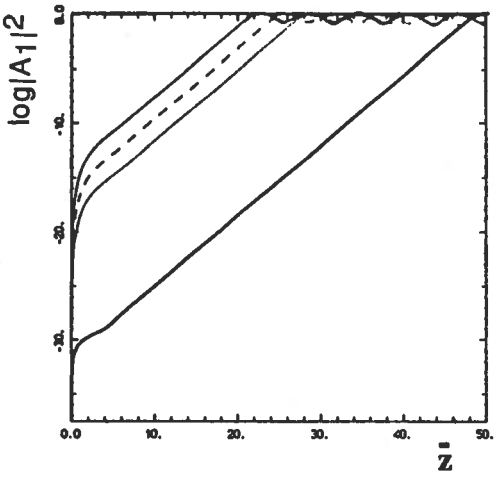

Fig.8 - Logarithm of the normalized first harmonic field intensity, plotted as a function of $\bar{z}$, for three different values of the initial sub-harmonic field intensity. See text for details.

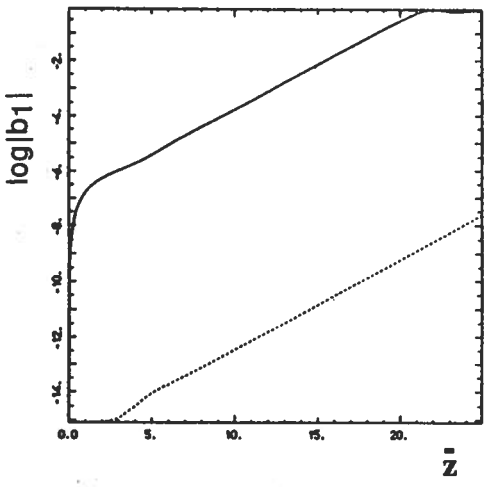

Fig.9 - Logarithm of the bunching amplitude $|b_1|$, plotted as a function of $\bar{z}$, for the two cases: with the sub-harmonic field (solid line) and without (dashed line). See text for details.

The incremental gain g, defined as $g = d\ln|A_1|^2/d\bar{z}$ (nepers), is plotted in Fig.10 versus z,- along the first part of the wiggler (40 wiggler periods): the dashed line gives the gain behaviour for the case of the start up from the numerical noise, i.e. without any sub-harmonic field, while the solid line corresponds to the three sub-harmonic input signals listed above. While the dashed line approaches quickly the standard value assumed during the exponential growth, given by $g=\sqrt{3}\cdot F_1^{2/3}(\xi)$, whose value is, for the present case, g=1.6 nepers, the incremental gain of the sub-harmonic driven case stays much more at higher values up to $\bar{z}\approx 6$, where the driving effect of the sub-harmonic field on the first harmonic radiated field becomes negligible with respect to the natural exponential growth of the latter.

In order to check that the SVEA approximation is satisfied, the first harmonic field phase ϕ_1 (we recall that $A_1=|A_1|e^{i\phi_1}$) must comes out to be a slowly varying function of $\bar{z}$: that is confirmed by the behaviour shown in Fig.11, where the solid line gives the phase $\phi_1(\bar{z})$ (modulus 2π) along the wiggler up to saturation, for the case of $|A_s^0|^2 = 0.2$. The dashed line gives the behaviour of $\phi_1(\bar{z})$ in absence of the sub-harmonic field ($|A_s^0|^2 = 0.$).

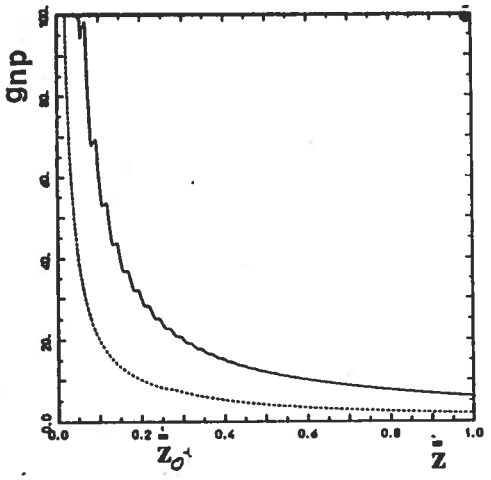

Fig.10 - Incremental gain (in nepers), plotted as a function of $\bar{z}$, for the two cases: with the sub-harmonic field (solid line) and without (dashed line).

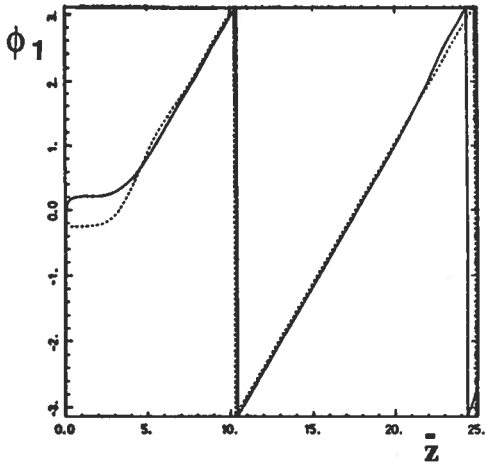

Fig.11 - First harmonic field phase ϕ_1, plotted as a function of $\bar{z}$, for the two cases: with the sub-harmonic field (solid line) and without (dashed line).

The phase space is plotted at $\bar{z}$=15 in Fig.12-a and at $\bar{z}$=20 (just before saturation, that occurs at $\bar{z}$=23) in Fig.12-b. It is interesting to note that in Fig.12-a the first harmonic field has already produced an energy modulation on the scale of its wavelength which is comparable to the spread induced by the sub-harmonic s=2: the atter stays fairly unaltered along the wiggler and superposed to the two buckets generated by the first harmonic.

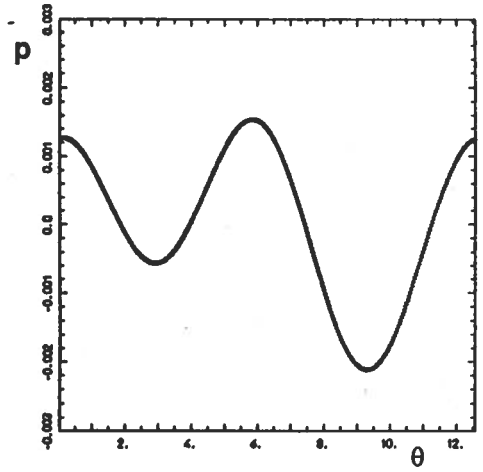

Fig.12-a - Phase space traced at $\bar{z}$=15 for the case of an initial sub-harmonic field intensity $|A_s^0|^2 = 0.2$.

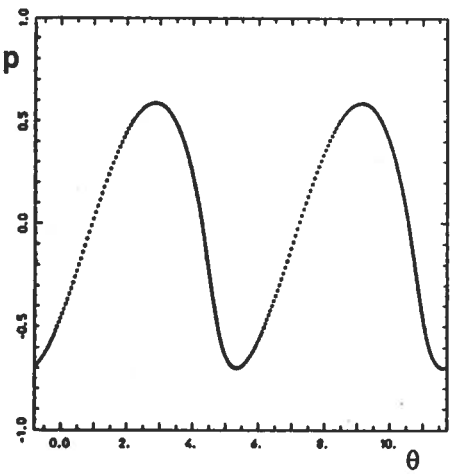

Fig.12-b - Phase space traced at $\bar{z}$=20 for the case of an initial sub-harmonic field intensity $|A_s^0|^2 = 0.2$.

Such an energy modulation on the scale of λ_s is seen as an incoherent beam spread by the first harmonic field, but its amplitude comes out to be quite negligible if compared to the coherent spread produced by the first harmonic field when the saturation is approached: that can be clearly seen in Fig.12-b (note the rescaling by a factor 300 of the p-scale), where the incoherent sub-harmonic spread is no more visible over the phase space. The intensity at saturation does not suffer, therefore, for the action of the sub-harmonic field and its value at saturation is, as usual in the cold-beam limit of the steady state regime, $|A_1|^2 \approx 1.2$ (i.e. $P_1 \approx \rho P_{beam}$).

As a last test, we analyzed the sensitivity of the FEL performances, within the SHOK scheme, against the presence of a first harmonic field signal in input and against the variation of the numerical noise generating the initial bunching (which, to some exent, can be considered as a physical Schottky noise).

The logarithm of the normalized first harmonic field intensity ($\log|A_1|^2$) is plotted versus $\bar{z}$ in Fig.13 (solid line), for the case of $|A_s^0|^2 = .2$ and no first harmonic field in input ($|A_1|^2=0$): the first harmonic intensity, starting at 38 orders of magnitude below the saturation level, reaches after 3 units of $\bar{z}$ the level 10^{-20}. When a signal on the first harmonic is injected in addition to the sub-harmonic field, at the levels $|A_1|^2=1\cdot10^{-29}$ and $|A_1|^2=1\cdot10^{-25}$, the behaviour of the first harmonic intensity is as shown by the dotted and the dashed lines, respectively: it comes out therefore that the driving action of the sub-harmonic field is unsensitive from a possible noise present on the first harmonic.

A similar conclusion can be reached about the sensitivity on the numerical noise: changing the machine espilon from (fairly indicative values) $\varepsilon_m\approx1\cdot10^{-15}$ to $\varepsilon_m\approx5\cdot10^{-8}$ (shifting from a 8 bytes floating point operation to a 4 bytes one), the initial bunching, present in the phase space because of the intrinsical straggling of the particle distribution, grows by the same quantity.

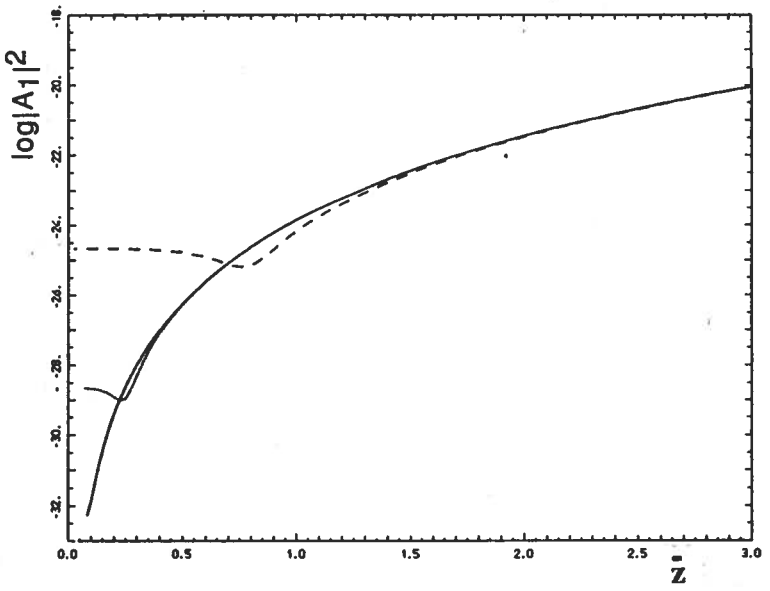

Fig.13 - Logarithm of the normalized first harmonic field intensity.plotted as a function of $\bar{z}$ for three different values of the initial first harmonic intensity.See text for details.

The first harmonic field intensity starts therefore from a higher value, whose order of magnitude can be easily computed using eq. 9-c) at the first order of approximation by: $|A_1|(\bar{z}=\delta\bar{z}) \approx F_1(\xi)\cdot|b_1^0|\cdot\delta\bar{z}$, where $|b_1^0|$ is the initial bunching amplitude. Recalling that in the present case the integration step $\delta\bar{z}=4\pi\rho/100=2.5\cdot10^{-4}$ and $F_1(\xi)=.8$ we obtain $|A_1|^2(\bar{z}=\delta\bar{z}) \approx 4\cdot10^{-38}$ for the lower ε_m and $|A_1|^2(\bar{z}=\delta\bar{z}) \approx 1\cdot10^{-22}$ for the higher one. However, the evolution of the first harmonic field

intensity is scarcely dependent on the starting bunching amplitude, as can be deduced from the lines plotted in Fig.14, where the solid line gives the behaviour corresponding to the lower $|b_1^0|$ value and the dotted one corresponds to the higher $|b_1^0|$. The difference of 15 orders of magnitude in the starting field intensity values is strongly reduced, after a few units of $\bar{z}$, down to two orders of magnitude. The corresponding incremental gain behaviours are plotted in Fig.15 for the two cases.

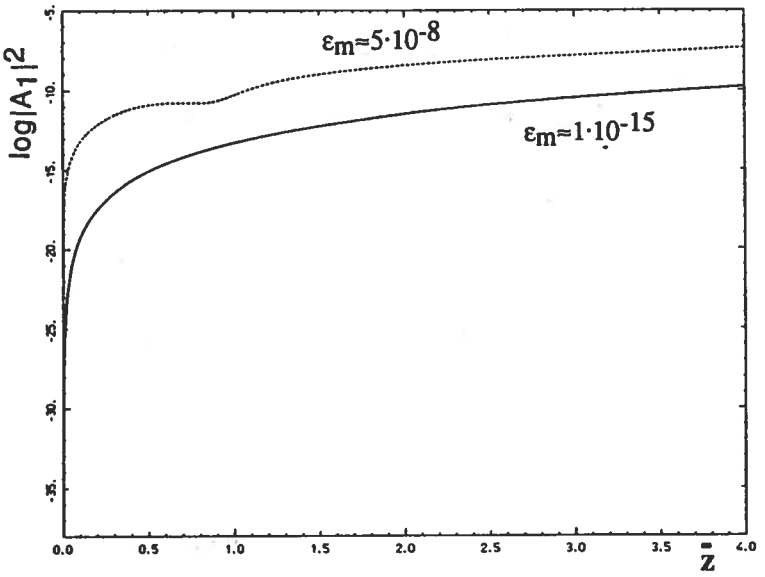

Fig.14 - Logarithm of the normalized first harmonic field intensity.plotted as a function of $\bar{z}$ for two different values of the machine epsilon.ε_m See text for details.

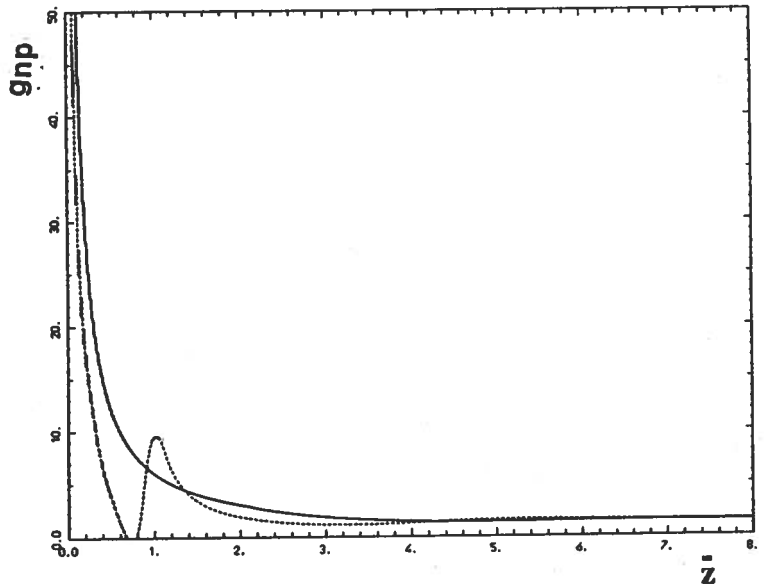

Fig.15 - Incremental gain (in nepers) corresponding to the two curves plotted in Fig.14

Other sub-harmonic orders have been considered. In principle it can be shown that the index s can be given by the ratio of any pair of integer numbers, s = n/m: the periodicity will be given anyway by n wiggler periods. In fact, the electrons slippage m sub-harmonic wavelengths λ_s (with respect to the sub-harmonic field) every n wiggler periods. N first harmonic buckets will still be needed to simulate one sub-harmonic bucket.

However, we analyzed still only the third sub-harmonic case, i.e. s=3. An experimental application of the fifth sub-harmonic will be treated later on in the last section.

We used again the same values for the wiggler-beam parameters as the ones listed above for the case of the second s=2 sub-harmonic.

The trajectory in the phase space of an electron started from the point (θ=.05236 rad, p=0) is plotted in Fig.16, for the case of $|A_s^0|^2$ = .2: the trajectory still exhibits, as the s=2 case, a slow drift in the phase θ, with large oscillations in p and small oscillations ($1 \cdot 10^{-5}$ rad) in phase. Now the macro-periodicity of the sub-harmonic action is no more (as in the case s=2) one wiggler period, but 3 wiggler period, i.e. one unit of N_s, as can be observed by the dotted and the dashed lines plotted in the figure, which show the particle position in the phase space at the end of each wiggler period (the dotted one) and every three wiggler periods (the dashed one).

The same effect can be observed looking at the behaviour of p_{max}, the maximum p value over the phase space, which is plotted (solid line) in Fig.17 along 30 wiggler periods (N_s=10): here again the dotted line connects the values assumed by p_{max} at the end of each wiggler period, while the dashed line connects the values of p_{max} at the end of each group of three wiggler periods (i.e. every unit of N_s).

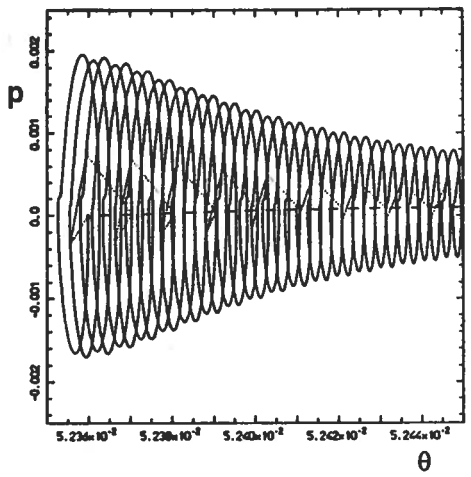

Fig.16 - Phase space trajectory for a test particle starting at z̄=0 from the point (θ=.05236 rad, p=0.), in the third s=3 sub-harmonic mode of operation. See text for details.

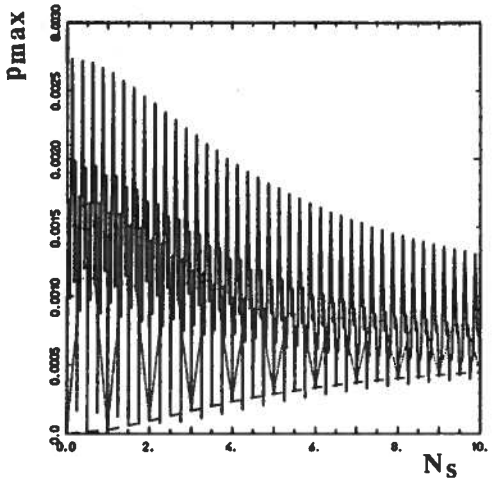

Fig.17 - Maximum value of p over the phase space plotted (solid line) along 30 wiggler periods, i.e. N_s=10., for the third s=3 sub-harmonic case. See text for details.

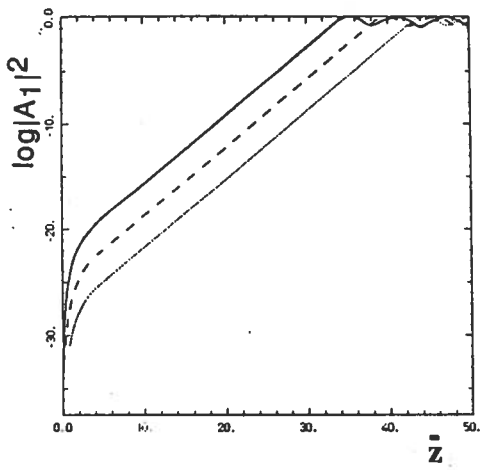

Fig.18 - Logarithm of the normalized first harmonic field intensity, plotted as a function of $\bar{z}$, for three different values of the initial sub-harmonic field intensity., for the third s=3 sub-harmonic case. See text for details.

The behaviour of the normalized intensity $|A_1|^2$ of the first harmonic field is shown in Fig.18, where the quantity $\log|A_1|^2$ is plotted for three different initial values of the sub-harmonic normalized field intensity: $|A_S^0|^2 = .2$ the solid line, $|A_S^0|^2 = .02$ the dashed line and $|A_S^0|^2 = .002$ the dotted one. The first harmonic field reaches saturation after $\bar{z}\approx 35$ starting from zero. The corresponding incremental gain g is plotted up to $\bar{z}=2.5$ in Fig.19. The crossed line shows the incremental gain of the first harmonic field growing from the numerical noise (i.e. without any sub-harmonic input signal): after a first "numerical" spike it reaches quickly the standard steady state value g=1.6 nepers (as reported above). On the contrary, the lines corresponding to the presence of a sub-harmonic field show, after the first unavoidable "numerical" spike which is common for all the lines, a large peak due to the driving effect of the sub-harmonic field: for the case $|A_S^0|^2 = .2$, the peak reaches the relevant value of 100 nepers!

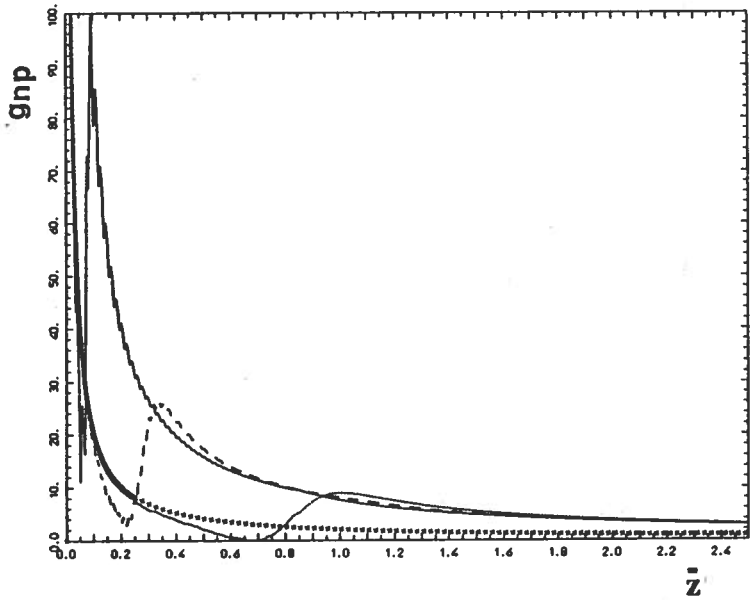

Fig.19 - Incremental gain (in nepers), plotted as a function of $\bar{z}$, for the two cases: with the sub-harmonic field (solid line) and without (dashed line). See text for details.

The evolution of the corresponding phase space is shown in Fig.20-a to 20-e for the case of $|A_S^0|^2 = .02$: the phase space are traced at the end of the first wiggler period (Fig.20-a), at the end of the third wiggler period when $N_S=1$ (Fig.20-b) and at the points $\bar{z}$= 30, 34 and 38 (Fig.20-c-d-e respectivley), just before saturation. It is clearly visible the progressive onset of the energy modulation produced by the first harmonic field which is driven by the energy modulation induced

by the sub-harmonic field: the single initial sub-harmonic bucket splits up into three first harmonic buckets, whose energy modulation amplitude continously grows (note the renormalization applied on the p scale) and finally is transformed into a phase modulation, i.e. into a bunching (Fig.20-e).

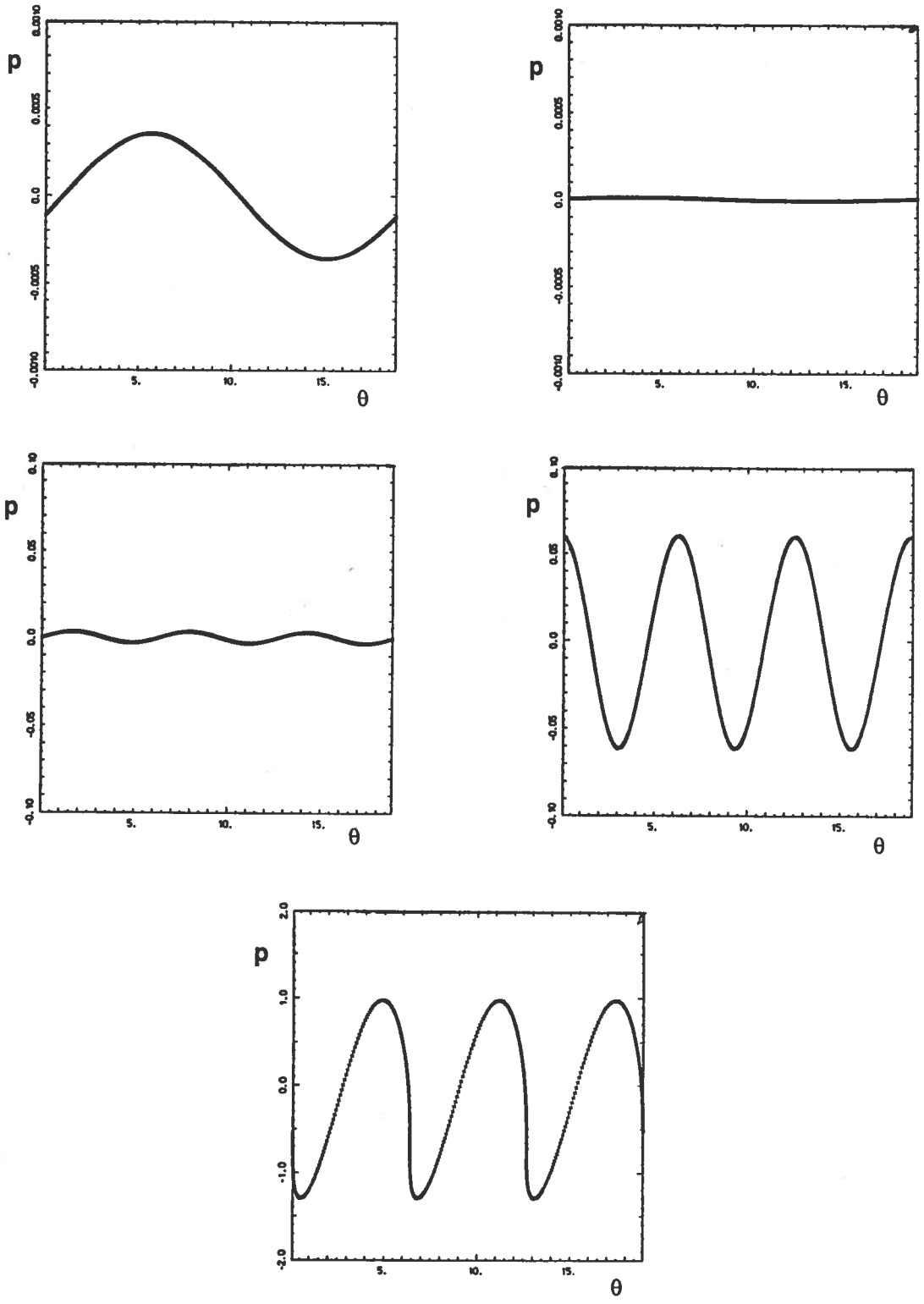

Fig.20-a to 20-e - Phase spaces for the third s=3 sub-harmonic case, traced at the end of the first wiggler period (a), at the end of the third wiggler period, where N_s=1 (b) and before saturation at the points $\bar{z}$= 30,34 and 38 (c-d-e respectivley).

3 - Some possible SHOK experiments

Although the applicability of the SHOK scheme covers the whole e.m. spectrum from the micro-waves up to the XUV rays, the availability in the near future of intense electron beams (some hundrets of A peak current) of high quality (rms normalized emittance in the range $1 \div 10 \cdot 10^{-6}$ m·rad) make feasible single pass high gain FEL's in the spectral region from 100 down to 5 nm of radiation wavelength (photon energy between 20 and 200 eV), where no coherent input signals are at present available. The full exploitation of the SHOK scheme lies therefore, in our opinion, within that spectral region, where the lacking of input signal can be overcome via the utilization of sub-harmonic input signals at higher wavelengths, to drive high gain FEL's in the X-VUV spectrum.

The recent developments of the frequency multiplication devices, applied to the high peak power Nd-YLF lasers, indicate that it will be possible to produce high peak power pulses in the VUV wavelength domain. A new laser system based on a mode locked ND-YLF frequency doubled laser produces 10 mJ pulses at a repetition rate of 1 kHz with a peak power of 200 MW over 50 ps, at a wavelength λ=532 nm. By means of a cascade of two 2-nd harmonic generator BBO crystals the green light is converted down to a wavelength of λ=133 nm with a total efficiency around the 10%. Laser puses in the VUV wavelength range at a peak power of 10 MW are in this way foreseen[16].

The anticipated availability, within the ARES project context, of high brightness electron beams gives us, as a natural choice, the opportunity to enlist in the following table the parameters of a typical "base" SHOK experiment, to be performed at the ARES facility: a further example for an "extended" SHOK experiment will be presented in the next section. The chosen sub-harmonic is the third one, s=3.

Table 1 - Base SHOK experiment parameters

Electron Beam	T = 530 MeV	I = 400 A	$\varepsilon_n = 8 \cdot 10^{-6}$ m·rad	σ_{beam}=190μm
Sub-harm. Laser		s = 3	λ_s = 133 nm	Z_0 = 1.7 m
Wiggler	λ_w = 3 cm	B_w = .75 T	ρ = .0016	λ_r = 44 nm

The radiated field power P at λ_r=44 nm is plotted as a function of the wiggler length in Fig.21. The saturation level is reached after 27 m of wiggler at 400 MW of peak power, starting without any input signal on the 44 nm wavelength field and with 10 MW of input signal on the 133 nm laser beam, which corresponds to a normalized sub-harmonic field intensity $|A_s^0|^2 = .03$. Since the rms beam radius within the wiggler is (in absence of ion focussing H=1) 190 μm, the radiated intensity, assuming an active optical guiding[18] of the electron beam on the radiated field, can be

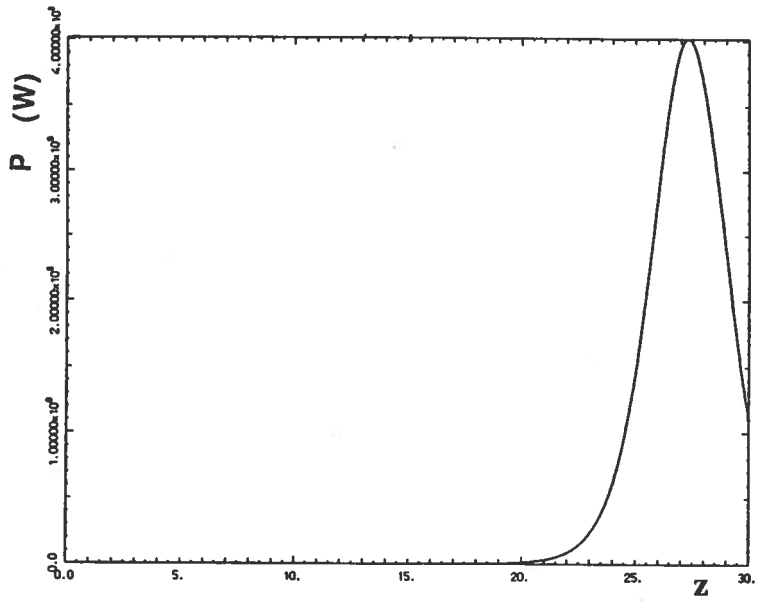

Fig.21 - Exponetial growth of the radiation at λ_r=44 nm, driven by a third sub-harmonic laser beam of 10 MW peak power. See text for details.

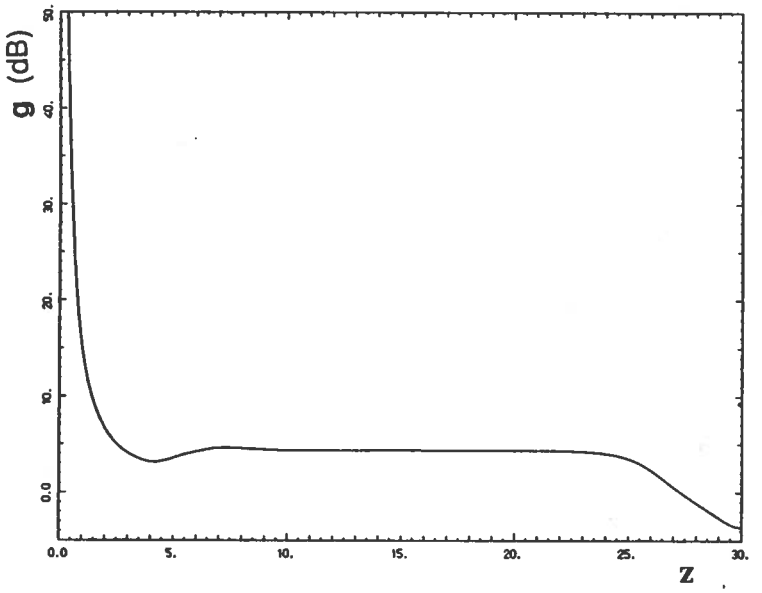

Fig.22 - Incremental gain g_{db} (in decibels) corresponding to the curve plotted in Fig.21. See text for details.

extimated at about $1 \cdot 10^{11}$ W/cm^2. The normalized beam emittance is in this case just compatible with the emittance threshold: the parameter $f_1=2\pi\varepsilon_n/(\lambda_r\gamma)$ comes out to be $f_1=1.1$. The final result is a frequency multiplication by a factor three of the ND-YLF laser beam together with an amplification by a factor 40 of its peak power. The incremental gain g_{db}, defined as dlog(P)/dz, is plotted in Fig.22: the plateau at 4 dB of the standard steady state exponential regime is anticipated by the large peak due to the driving effect of the sub-harmonic field. Since the electron bunches delivered by the ARES SC LINAC[17] are foreseen to be a few ps in time-length, a further compression of the 50 ps ND-YLF laser pulses could be envisaged, in order to push up the peak power of the sub-harmonic field at 133 nm. A 50 MW sub-harmonic signal will allow to reduce the wiggler length needed to reach saturation down to 23 m.

4 - Towards the "water window"

One of the main goal of the FEL facility under study at the ARES project is the generation of brigth coherent radiation at λ_r=5 nm, i.e. the construction of a device able to produce coherent soft X-rays at high peak power and within the so called "water window" at 50 Å (photon energy 248 eV).

A direct jump in frequency from the VUV light of the ND-YLF laser cited above up to the 50 Å X-ray radiation seems not feasibe via a simple SHOK scheme as presented in the past sections. At least one cascade with two or more jumps in frequency must be envisaged: a mixed scheme of SHOK + frequency multiplier appears to be mandatory.

Moreover, the electron beam must exhibits the best quality envisageable with the ARES SC LINAC under study: the parameters listed in the following table represent a typical set of values required to radiate at 5 nm. Note the low energy spread (made feasible by the low-frequency RF chosen for the SC LINAC), the high repetition rate and the respectable beam peak power $P_{beam}=3.28\cdot10^{11}$ W.

Table 2 - Beam requirements to radiate at the "water window"

T [MeV]	I [A]	ε_n [m rad]	$\Delta\gamma/\gamma$ [keV]	σ_{bunch} (ps)	rep.rate (kHz)
820	400	$3\cdot10^{-6}$	$\pm$ 250	.5	0.1÷1.

Since λ_r=5 nm is fairly the 25-th harmonics of λ_r=133 nm, a double jump in frequency by a factor 5 comes out to be the natural choice: however, as it has been illustrated in the past section, the efficiency of the SHOK scheme decreases with larger sub-harmonic orders s. Therefore a new "extended" SHOK scheme is necessary, as presented in the following, to assure the possibility to reach the water window without the need of extremely long wigglers. Such a new apparatus is based on two main properties of the SHOK scheme:

- The sub-harmonic laser beam is focussed in such a way to present a beam waist at the wiggler entrance: the defocussing part of the beam envelope inside the wiggler is the region of overlapping with the electron beam, where the sub-harmonic field induces a coherent energy spread to the beam.

- It has been shown that the total momentum transfer between the sub-harmonic optical field and the electron beam is negligible: the sub-harmonic field amplitude can be therefore assumed to be determined by the laser beam envelope behaviour, which is regulated by the laser optics in front of the wiggler.

In order to improve the efficiency of the sub-harmonic field in generating a coherent energy spread on the electron beam we can therefore envisage to add in front of the wiggler a few periods of what we call a "spreader", which is simply a wiggler whose period is scaled up by a factor s with respect to the period λ_w of the main subsequent wiggler. The spreader is then a wiggler whose first harmonic equals the sub-harmonic optical field wave, whose wavelength is $s\cdot\lambda_r$. It will be shown that the number of spreader periods can be small, of the order of a few units, in order to maximize the performances of the whole system.

The main wiggler is tuned to radiate at a first harmonic of λ_r=25 nm: the simultaneous growth of the fifth harmonic at λ_r=5 nm causes the electron beam to be bunched also on this wavelength scale. The subsequent injection of the bunched beam, after some meters of the main wiggler, into a radiator tuned on the 5 nm wavelength makes possible to obtain high peak power radiation at the water window: a lay-out of the whole apparatus is shown in Fig.23. The system wiggler+radiator is discussed in details elsewhere[7].

A matching condition for the beam trajectory imposes a continuity condition on the transverse velocity at the interface between the spreader and the wiggler, i.e. the amplitude of the $\beta\tau$'s in the spreader and in the wiggler must be equal: this requires that both have the same vector potential a_w. It follows that the peak magnetic field of the spreader B_w^{sp} must be 1/s times the peak field of the wiggler.

The previous considerations suggest a typical set of parameters, for the extended SHOK device, as reported in the following table.

Table 3 - Extended SHOK experiment parameters

Sub-harm. laser		s=5	P_{las}=10 MW		λ_s=125 nm	Z_0=.43 m
Spreader	λ_w^{sp}=20 cm	B_w^{sp}=.11 T	a_w^{sp}=1.48		N_{period} = 4	ρ^{sp}=.0034
Wiggler	λ_w=4 cm	B_w=.56 T	a_w=1.48	H=.5	σ_{beam}=92 μm	ρ=.002
Radiator	λ_w^R=2 cm	B_w^R=.41 T	a_w^R=.53	H^R=.1	σ_{beam}^R=50 μm	ρ^R=.001

The 1-d simulations have been performed integrating the SHOK equations 9) taking as initial conditions the output particles from the spreader, which is described via a set of standard FEL Compton equations whose first harmonic field is represented by the sub-harmonic laser beam. At the end of the main wiggler all the harmonics field intensities $|A_h|^2$ are set to zero, to reproduce the

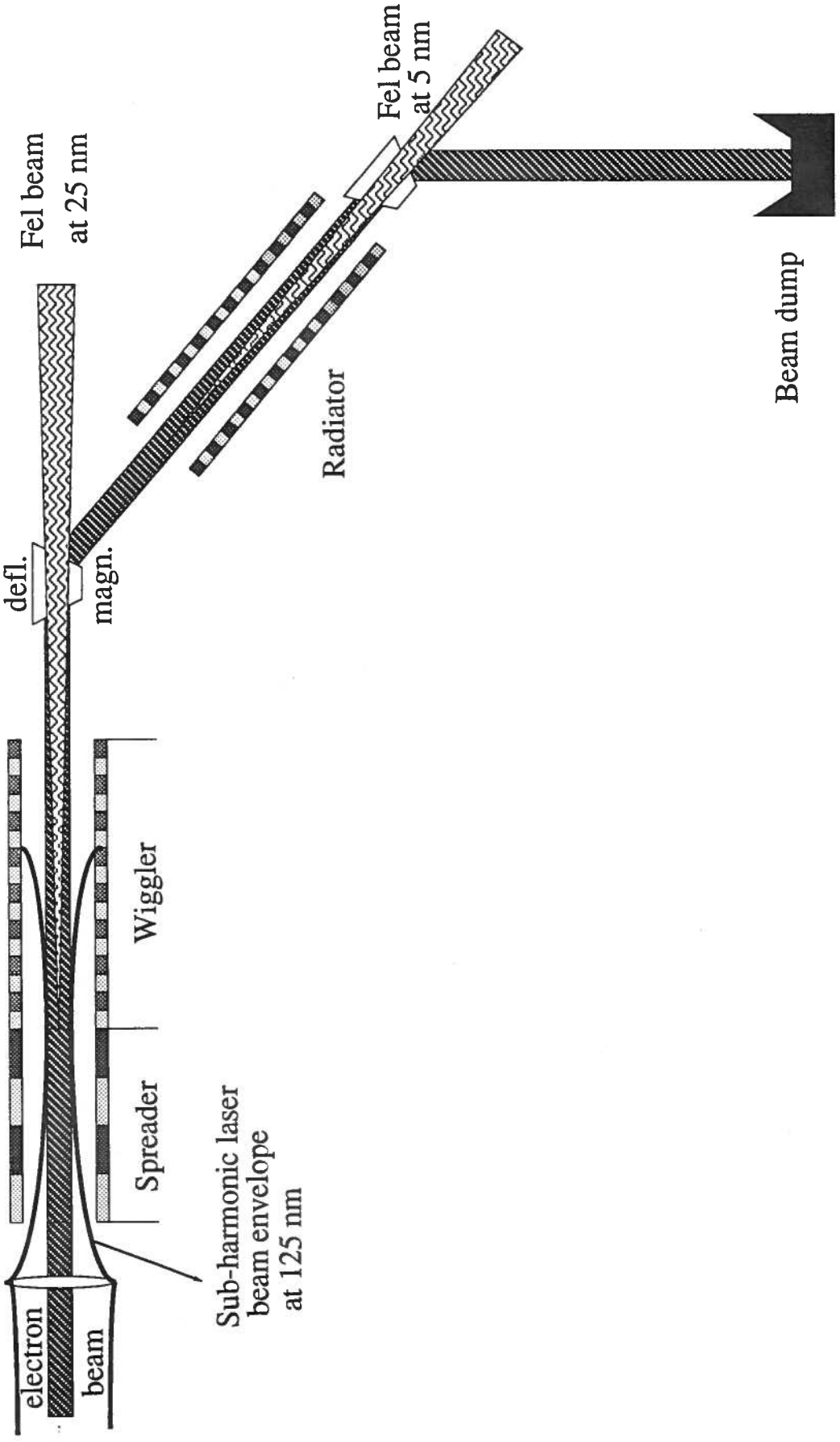

Fig.23 - Extended SHOK apparatus

discarding of the radiation and the injection of only the electron beam into the radiator (as described elsewhere[7,19] in major details).

In Fig.24 the radiation field power P is plotted along the cumulative length z of the system spreader+wiggler+radiator: the negative part of the z-axis corresponds to the .8 m of the spreader length, while the wiggler extends from z=0 up to z=17 m. The power plotted up to the wiggler end corresponds to the first harmonic field of the wiggler, i.e. to the radiation at 25 nm: the entrance of the radiator corresponds to z=17 m (although this could not be the real disposition, i.e. the radiator can be far apart from the wiggler). The power of the radiation at λ_r=5 nm grows in the radiator and reaches saturation after still 10 m of radiator length, at a power level of 360 MW, which corresponds to an intensity of $4.6 \cdot 10^{12}$ W/cm^2. A slight ion focussing effect has been applied both to the wiggler (with a reduction by a factor H=.5 of the betatron wavelength) and to the radiator (with H=.1). The input sub-harmonic laser power has been taken P_{las}=10 MW, while no input field has been injected on the wiggler first harmonic at 25 nm. The logarithm of the amplitude of the bunching parameters on the first wiggler harmonic $|b_1|$ and on the fifth one $|b_5|$ are plotted (solid and dashed line respectively) in Fig.25 as funtions of the dimensionless $\bar{z}$ up to the wiggler end at $\bar{z}$ =10.5: for larger $\bar{z}$ the same parameters $|b_1^R|$ and $|b_5^R|$ correspond to the radiator (since the beam is injected from the wiggler into the radiator, the condition $|b_1^R| = |b_5|$ must hold at the interface). The strong driving effect of the sub-harmonic field is clearly visible in the first part of the wiggler, where the bunching grows very rapidly from the initial noise level.

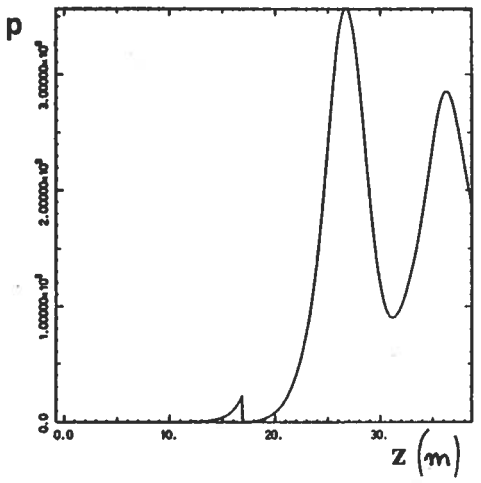

Fig.24 - Exponential growth of the λ_r=5 nm radiation power within the "extended" SHOK scheme (spreader+wiggler+radiator). See text for details.

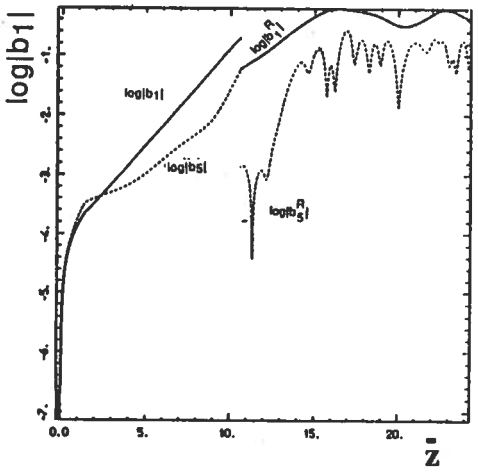

Fig.25 - Logarithm of the first harmonic $|b_1|$ and fifth harmonic $|b_5|$ bunching amplitude along the wiggler ($\bar{z}$<10.5) and the radiator ($|b_1^R|$ and $|b_5^R|$).

The phase spaces are plotted in Fig.26a-f at some positions along the whole system: the energy spread induced by the 4 spreader periods is evident from the phase space traced at z=0 (wiggler entrance, Fig.26-a). The phase space extends over 5 buckets of the λ_r=25 nm radiation, since the

sub-harmonic order is in this case s=5: the coherent spread is induced on the scale of the sub-harmonic wavelength. After 14 meters of wiggler length (Fig.26-b) the phase space still holds the energy modulation on the scale of the sub-harmonic wavelength, but the energy spread of the first harmonic at 25 nm sets up together with a slight modulation on the third harmonic at 8.3 nm, which further increases at the end of the wiggler (z=17 m, Fig.26-c, note the renormalization in the scale of p), until the sub-harmonic energy modulation is no more visible. The weak energy modulation on the wiggler third harmonic is still present at z=19 m (Fig.26-d), i.e. after 2 meters of radiator length, but at z=21.5 m (after 4.5 meters of radiator length, Fig.26-e) it has been overcome by the strong modulation in energy and phase given by the radiator first harmonic at 5 nm (wiggler fifth harmonic): note that the phase scale has been renormalized up to 25 buckets of the 5 nm wavelength, to take into account the jump in frequency from the wiggler to the radiator. Finally, at z=24 m after 7 meters of radiator length, the phase space traced in Fig.26-f just before saturation shows how the energy modulation has been converted completely into a phase modulation (i.e. a bunching) on the first harmonic of the radiator: 25 bunches can be counted all over the phase space, with a residual weak energy modulation on the scale of the 25 nm wavelength and a negligible modulation on the 125 nm wavelength scale.

5 - Conclusions

The results of this preliminary study on the coupling between an electron beam and a sub-harmonic field in a wiggler show that the energy modulation induced on the beam is adequate to start up an exponential gain regime in absence of any pre-bunching of the beam neither any coherent input signal on the wiggler first harmonic: such a scheme can be of great usefulness in all the single pass high gain FEL's which suffer for the lacking of an appropriate source of coherent input signals (in particular the X-VUV FEL's).

Further studies are in course on this subject, in order to explore the full potentiality of the SHOK scheme and to better understand the driving effect of the sub-harmonic optical field on the bunching and on the first harmonic field intensity: a collective variable description could clarify the role plaied by the sub-harmonic signal and its quasi-low-gain coupling with the electron beam.

3D simulations are also needed to investigate how the distributions in the transverse phase spaces of both the electron beam and the two radiation beams (the sub-harmonic and the first harmonic one) can affect the performances of the SHOK scheme.

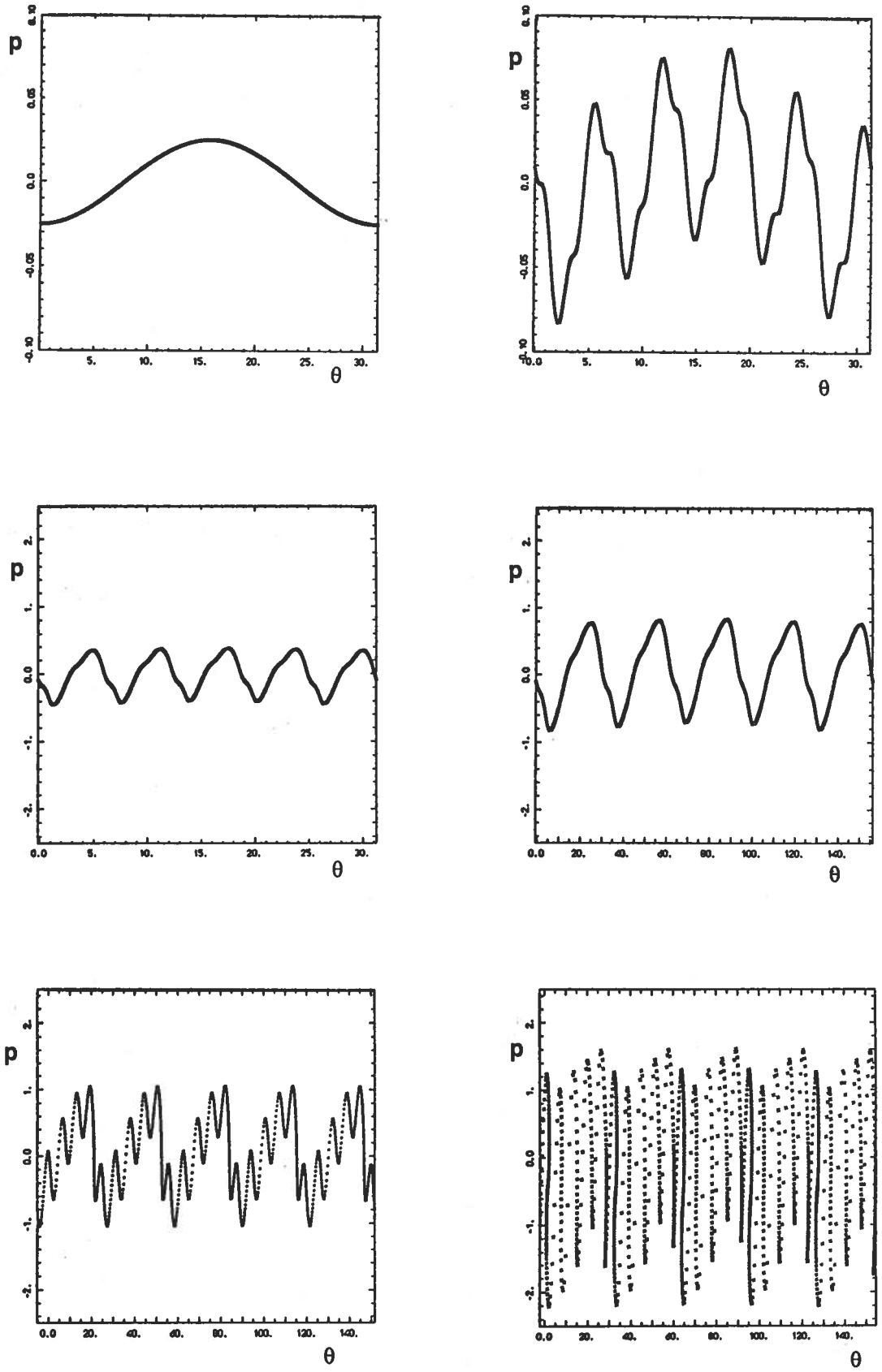

Fig.26a-f - Phase space plotted at some positions along the "extended" SHOK device (spreader+wiggler+radiator). See text for details.

Acknowledgments

We are really very much indebted to G.Vignola and M.Castellano for all the claryfing discussions on the driving action of the sub-harmonic field. We would like to thank also A.Ghigo for all the useful informations about the new laser systems in the VUV range. Our gratitude is due to W.A.Barletta and A.M.Sessler for having stimulated our attention to the subject of XUV FEL and for their encouragement and support in proposing the XUV FEL experiments at the ARES SC LINAC facility.

References

(1) J.C. Goldstein - Proc. ICFA Work. on low emittance e^-e^+ beams, Brookhaven, March 1987, p.180.
(2) C.Pellegrini - Proc. Int. Work. on coherent and coll. prop. in the interactions. of rel. electrons and e.m. rad., Como (Italy), Sept.1984, p.127.
(3) J.B. Murphy - Proc. ICFA Work. on low emittance e^-e^+ beams, Brookhaven, March 1987, p.197.
(4) R.Bonifacio et al. - Proc. of the INFN Int. School on Electromagnetic Radiation and Particle Beams Acceleration - Varenna (Italy), June 1988, p.35.
(5) R.Bonifacio et al. - Proc. of the INFN Int. School on Electromagnetic Radiation and Particle Beams Acceleration - Varenna (Italy), June 1988, p.259.
(6) R.Bonifacio, L.DeSalvoSouza, P.Pierini and E.T.Scharlemann - Proc. Int. FEL Conference 1989.
(7) L.Serafini et al., INFN rep. LNF-90/TC (R), March 1990.
(8) C.Pellegrini - NIM **A227** (1980) p.177.
(9) R.Coisson - Part. Accelerators, **11** (1981) p.245.
(10) D.F.Alferov and E.G.Bessonov - Sov. Phys. Tech. Phys. **24** (4) 1979, p.450.
(11) R.Bonifacio, C.Pellegrini and L.M.Narducci - Opt. Comm. **50** (1984) p.373.
(12) E.T.Scharlemann - "Wiggle plane focussing in a linear wiggler" - LLNL Report UCRL-92429.
(13) W.A.Barletta and A.M.Sessler - Proc. of the INFN Int. School on Electromagnetic Radiation and Particle Beams Acceleration - Varenna (Italy), June 1988, p.211-220.
(14) J.B.Murphy, C.Pellegrini and R.Bonifacio - Opt. Comm. **53** (1985) p.197.
(15) R.Bonifacio, F.Casagrande and C.Pellegrini - Opt. Comm. **61** (1987) p.55.
(16) A.Ghigo - Sistemi Laser per esperimenti FEL VUV - Memo ARES 35, Internal rep. LNF, Frascati, March 1990.
(17) "Ares Design Study (The Machine)" - Report LNF-90/005(R), January 17th 1990, Frascati.
(18) E.T.Scharlemann, A.M.Sessler and J.S.Wurtele, Proc. of Int. Work. on Coherent and Collective Prop. in the Int. of rel. electr.and e.m.Rad., Como, Italy, Sept. 1984.,p.29.
(19) M.Billardon, R.Coisson and Y.Lapierre - Appl. Phys. B39 (1986) 9.